CHAPTER TWO

Risk Analysis for Hurricanes Accounting for the Effects of Climate Change

Alessandro Contento, Hao Xu, Paolo Gardoni
Department of Civil and Environmental Engineering, MAE Center, University of Illinois at Urbana-Champaign, Urbana, IL, United States

2.1 Introduction

In the last decades, the devastating impact of hurricanes revealed the vulnerability of large areas of the US East and Gulf coasts to this natural hazard. The high toll paid in terms of human lives and the structural damage due to different storm occurrences raised the awareness about hurricanes. The importance of developing mitigation and adaptation strategies to reduce the loss of lives and properties due to hurricane occurrences was formally recognised at the Federal level with the National Windstorm Impact Reduction Act Reauthorisation of 2015 (PL 114-52). The resulting National Windstorm Impact Reduction Program (NWIRP), a joint Program of several Federal agencies led by the National Institute of Standards and Technology (NIST), has as its main objectives the improvement of the understanding of windstorms and the development of cost-effective mitigation strategies to reduce their impact.

Additionally, the impact of hurricanes may be exacerbated by climate change and the population growth of coastal communities (Murphy et al., 2018). Understanding how climate change affects the behaviour of extreme storms, and in particular of hurricanes, is a challenging task. Large-scale average climate is typically simulated using Atmospheric General Circulation Models (AGCMs). The main issues when looking at climate change using AGCMs are: (1) the identification of events is challenging when events have limited temporal and spatial extension as in the case of hurricanes, and (2) the AGCMs typically have difficulties in capturing the underlying local physics. Because of these issues, identifying trends (e.g., possibly due to climate change) in hurricanes is more complex than identifying trends in large environment characteristics such as changes in

Climate Adaptation Engineering
https://doi.org/10.1016/B978-0-12-816782-3.00002-4

temperature. The Intergovernmental Panel on Climate Change Fourth Assessment Report (IPCC AR4) (IPCC, 2007) was able to show that high-resolution AGCMs can reproduce approximately the frequency and distribution of hurricanes. More recently, the Intergovernmental Panel on Climate Change Fifth Assessment Report (IPCC AR5) (IPCC, 2013) showed that high-resolution AGCMs (LaRow et al., 2008; Zhao et al., 2009; Strachan et al., 2013) can simulate the year-to-year count variability of hurricanes for given observed sea-surface temperatures (SSTs). However, in both cases, such models underestimated the storm intensity. New models with improved parameterisations and higher resolution, such as the one presented by Mizuta et al. (2012), seem to be capable of providing an accurate distribution of the annual storm occurrences as well as simulating events with intensities comparable to those observed.

Although a general consensus has not been reached, the majority of the numerical analyses (e.g., Camargo, 2013; IPCC, 2013; Knutson et al., 2015) suggests an increase in the global mean intensity of the hurricanes, the number of the most intense occurrences, and the precipitation rate. Conversely, the global frequency of hurricanes is expected to slightly decrease or remain unaltered. A probable trend detected in the results of the numerical analyses is the poleward migration of the locations where the hurricanes land (Kossin et al., 2016). Another interaction between hurricanes and climate change is the potential effect of sea-level rise that sets a higher starting level for storm surge and may increase the extent of the vulnerable areas.

Foreseeing an increase in the already consistent damage due to hurricanes clearly motivates the need for long-term mitigation and adaptation strategies. For natural hazards, the terms 'mitigation' and 'adaptation' may assume different meanings than those in the literature on climate change. Consequently, there is the need to clarify how these terms are used and what is intended for mitigation and adaptation strategies when talking about the natural hazards affected by climate change. Independently from the choice of the adopted terminology, the choice of the mitigation and adaptation strategies should be based on risk assessment analyses. Such analyses require the use of a specific risk analysis framework that, starting from the modelling of the hazard, allows the propagation of uncertainties up to the loss estimation (Contento et al., 2017).

A framework for the risk analysis for hurricanes needs to consider three fundamental aspects of hurricanes (wind, rainfall, and storm surge), should be able to account for the effects of climate change, and should adopt wind, rainfall, and storm-surge models that are computationally efficient. Several wind and rainfall models in the literature can account for the effects of

climate change and are computationally efficient (Vickery et al., 2000b; Emanuel et al., 2006; Mudd et al., 2017). However, currently models for storm surge that can account for the effects of climate change are generally computationally inefficient (Jelesnianski et al., 1992; Westerink et al., 1994). A few models that are computationally efficient (e.g., Irish et al., 2008; Jia and Taflanidis, 2013) are empirical, and their functional forms lack physical meaning and are not based on the understanding of the underlying physical phenomena. Moreover, because of the specific formulation used to construct such models, it is generally not possible to incorporate both results from simulations and historical observations in the model calibration. Consequently, there is the need to define efficient models that can account for the effects of climate change while capturing the physics of the phenomena and can incorporate data from both simulations and historical observations.

After clarifying the meaning of mitigation and adaptation strategies in the present context, the chapter summarises a general framework for hurricane risk analysis that can be used to compare mitigation and adaptation strategies. The chapter describes each step of the framework and the specifications of the models that are needed. The chapter also presents a novel probabilistic model proposed by Contento et al. (2018) to model the storm-surge height. Such a model accounts for the underlying physics of the phenomena, is computationally efficient, and overcomes the limitation of the available empirical models on the use of different data. Several examples of storm-surge height predictions show the ability and accuracy of the model. Lastly, the chapter suggests possible uses of the presented model for the evaluation of different mitigation and adaptation strategies.

Section 2.2 proposes a consistent use of the terms mitigation and adaptation when talking about natural hazards affected by climate change. Section 2.3 presents the general framework for hurricane risk analysis. Section 2.4 reviews the existing formulations for storm surge and presents the probabilistic model proposed by Contento et al. (2018). Finally, Section 2.5 presents how the information provided by the hurricane risk analysis can be used.

2.2 Mitigation Versus Adaptation

The terms ‘mitigation’ and ‘adaptation’ are widely used in the literature related to natural hazards and climate change. However, the meaning of mitigation and adaptation is inconsistent between the literature related to

natural hazard and the literature on climate change. Looking at the dictionary definition, mitigation is "the action of reducing the severity, seriousness, or painfulness of something" (Stevenson, 2010). When referred to natural hazard and climate change, the word mitigation assumes different meanings. For natural hazards, mitigation refers to the reduction of the impacts (or consequences) of physical hazards through the reduction of exposure or vulnerability. Since natural hazards traditionally could not be influenced by human interventions, the focus has been only on reducing of the effects of the physical phenomenon and not on changing the intensity or the likelihood of occurrence of the phenomenon itself. Since climate change is at least in part due to human activities, mitigation typically focuses on the source of climate change and refers to the reduction of greenhouse emissions and the enhancement of the sinks of such gasses (IPCC, 2013). The dictionary definition of adaptation refers to "adjust[ing] to new conditions" (Stevenson, 2010). The term adaptation is typically not used in the context of natural hazards. In the context of climate change, adaptation typically refers to the efforts towards ameliorating the consequences of climate change by adjusting to new climate conditions and their effects (IPCC, 2013), see also Chapter 1.

For both natural hazards and climate change, mitigation and adaptation strategies can be defined at two different levels: (i) the level of the built or modified natural environment, and (ii) the community level. When looking at hurricanes as an example of natural hazards, mitigation strategies for the built or modified natural environment might consist in reducing the vulnerability of structures and infrastructure to high wind, torrential rain, and storm surge. At the community level, mitigation might include education actions meant to increase awareness and preparedness, and the adoption of building codes and regulations for land use. As an extreme measure, mitigation strategies may culminate in relocation (Olshansky, 2018). When looking at climate change, mitigation strategies are only defined at the community level. Examples are activities that increase carbon stocks, reduction of direct agricultural emissions, and prevention of deforestation and degradation of high-carbon ecosystems. The adaptation strategies for climate change are the set of actions meant to reduce the consequences of climate change and, as such, they correspond to the mitigation strategies for natural hazards.

As a result, the same activity (like erecting a levee) is called a mitigation strategy when considering hurricanes as natural hazards, while it is called an adaptation strategy in the context of climate change. Consequently, we need to clarify how these terms are used when talking about the natural hazards

affected by climate change. We propose to use the term mitigation to refer to the activities targeted at influencing climate change insofar it affects the natural hazards. We also propose to use the term adaptation to refer to the activities targeted at reducing the impact of natural hazards (influenced or not by climate change). In particular, we propose the use of the terms 'environmental adaptation' and 'human adaptation' to differentiate between adaptation measures that modify the environment (built or natural) and those that involve changes in human activities (Cooper and Pile, 2013).

Given the inevitability of climate change, all coastal communities will be forced to adopt adaptation strategies. While farsighted legislators may anticipate adaptation strategies, adaptation and will most likely follow hurricane-induced disaster occurrences in the form of long-term postdisaster recovery (Olshansky, 2018). Be it before or after a disaster, the choice of adaptation strategies should be based on the results of risk analyses. Such risk analyses necessitate the use of a comprehensive framework, which combines the different aspects of the hazard (e.g., wind, rainfall, and storm surge in the case hurricanes), accounts for climate change, and adopts wind, rainfall, and storm-surge models that are computationally efficient.

2.3 Framework for Risk Analysis

This section presents a general framework for hurricane risk analysis that is based on the literature and current practice. The presented framework involves four steps. Step 1 models the hurricane activity and simulates synthetic storms needed to derive the landfall statistics. Step 2 models the three aspects of the hazard and provides possible hazard scenarios. Step 3 models damage, predicts losses, and provides the corresponding distributions and probabilities of exceedance. Step 4 uses the information coming from the previous steps for the comparison and development of mitigation and adaptation strategies. The framework accounts for the underlying uncertainties from the hazard up to the loss estimation and the development of mitigation and adaptation strategies (Gardoni, 2017; Murphy et al., 2018). To allow for both short- and long-term analyses, each step directly or indirectly can account for the effects of climate change. Additionally, the framework adopts models that are mostly physics based (which is important to improve the applicability of the models to cases other than those used in the model calibration) and computationally efficient (which is important given the necessity of large numbers of simulations).

The remaining of this section briefly describes each step. Section 2.4 reviews the existing formulations for storm surge and presents the probabilistic model proposed by Contento et al. (2018) that can be used in Step 2. Section 2.5 presents the details of Step 4 describing how the information coming from the first three steps can be used in the development of mitigation and adaptation strategies.

2.3.1 Hurricane Activity Models (Step 1)

Developing a hurricane model and simulating hurricane occurrences is the first step of a hurricane risk analysis (Lin et al., 2012, 2014). Hurricane models are needed to simulate synthetic storms to be used in a Monte Carlo simulation for deriving the landfall statistics (i.e., the hurricane characteristics at landing). Since hurricane models are function of variables depending on climate change, such as SSTs, the effects of possible mitigation strategies will directly affect the landfall statistics.

There are several models available in the literature to describe the genesis, track, and intensity of hurricanes (e.g., Russell, 1971; Vickery et al., 2000b; Emanuel et al., 2006; Lee and Rosowsky, 2007). These models can be empirical (Neumann, 1991, Vickery and Twisdale, 1995), mixed empirical and physics based (Vickery et al., 2000b, Powell et al., 2005, Lee and Rosowsky, 2007), or physics based (Emanuel et al., 2006). In this chapter, we distinguish between empirical and physics-based models. We call empirical models those constructed by fitting an arbitrary model form to simulated or field data. In contrast, physics-based models are those constructed based on the understanding of the underlying physics of the phenomena. We also distinguish between deterministic and probabilistic models. Deterministic models do not account for the underlying uncertainties, while probabilistic models do. Empirical model could be either deterministic (e.g., when the parameters in the model calibrated from the data are fixed at their mean values), or probabilistic. Similarly, physics-based models can be either deterministic (e.g., when the models are constructed purely based on first principles) or probabilistic (e.g., when data are used in addition to the first principles to develop the model and the uncertainties are captured in the final model form). Each of the three kinds of model available in the literature for hurricane activities has strengths and limitations; extensive reviews on hurricane models can be found in Vickery et al. (2009a) and Lin et al. (2014).

Among the available models, the one presented by Vickery et al. (2000b), and improved by Vickery et al. (2009b), is well-suited for analyses that require a high number of simulations. Although this model proposes an empirical tracking model, it is still capable of retaining information about the physics of the problem through a proper choice of the regressors. This model was used by Mudd et al. (2014) for analyses that include the effects of climate change using projections of SSTs.

2.3.2 Hazard Scenario Models (Step 2)

After the simulation of the hurricane characteristics, hazard models are needed to simulate the resulting wind, rainfall, and storm surge. For the wind aspect, different wind profiles, either parametric (Holland, 1980; Holland et al., 2010; Chavas et al., 2015) or nonparametric (Thompson and Cardone, 1996; Kepert, 2010) are available in the literature. Generally, the surface wind field is obtained as the combination of an axisymmetric surface wind field and a background wind field.

The axisymmetric surface wind field is derived from a gradient wind field model (e.g., Batts et al., 1980; Holland, 1980; Jelesnianski et al., 1992; Emanuel, 2004; Emanuel and Rotunno, 2011). Such derivation can be done either by accounting for the surface friction with empirical correction terms, such as an empirical surface wind reduction factor (Schwerdt et al., 1979; Batts et al., 1980; Georgiou, 1985; Vickery et al., 2000a; Powell et al., 2003) and an inflow angle (Bretschneider, 1972), or using boundary layer models (e.g., Thompson and Cardone, 1996; Vickery et al., 2009b; Kepert, 2010). Boundary layer models provide the mean wind speed profile in the hurricane boundary layer. Such models tend to be more accurate and computationally demanding than those that use empirical correction terms. They are usually nonparametric with only a few exceptions. One example of a parametric model was developed by Vickery et al. (2009b) that empirically modelled the variation of the mean wind speed with height.

The background wind field is typically modelled as a function of the hurricane's translational velocity having the same direction and a proportional intensity. Some formulations use the full value of the hurricane's translational velocity (e.g., Powell et al., 2005; Mattocks and Forbes, 2008; Vickery et al., 2009b), while others use reducing factors that vary in each formulation (e.g., Jelesnianski et al., 1992; Phadke et al., 2003; Emanuel et al., 2006; Lin et al., 2012).

The rainfall models available in the literature are mostly empirical models (Lonfat et al., 2007; Tuleya et al., 2007; Mudd et al., 2017) based on the rainfall climatology and persistence model (R-CLIPER). These models are usually developed using recorded rainfall data associated with hurricane events. Langousis and Veneziano (2009) developed a model of tropical cyclone rainfall based on the vertical outflow of water vapour from the tropical cyclone boundary layer. Only a few studies in the literature proposed coupled studies for wind and rainfall (e.g., Mudd et al., 2017).

For the storm surge, the common practice is the use of models such as the sea, lake, and overland surges from hurricanes (SLOSH) model (Jelesnianski et al., 1992) or the advanced circulation (ADCIRC) model (Westerink et al., 1994). Usually these models have either low accuracy or high input requirements, are complex and time consuming to develop for a specific site, and are computationally expensive. Those that have low accuracy (but are easier to develop and more computationally efficient) are most suitable to forecast the storm surge promptly in the case of the occurrence of a real hurricane. Those that have higher accuracy are preferred for detailed probabilistic analyses. However, their computational inefficiency makes them unsuitable for performing the high number of simulations typically required by probabilistic analyses. Especially for the comparisons between possible climate change scenarios where multiple analyses are needed, simplified models fitted to available data are a viable alternative. However, such models available in the literature and sometime also referred to as 'metamodels' or 'surrogate models' (Jia and Taflanidis, 2013; Kim et al., 2015; Jia et al., 2016) have some limitations. First, the models can only be trained using data coming from either simulations or historical records. Second, they are only able to predict the storm surge at the same locations of the data used to calibrate the model. Section 2.4 focuses explicitly on this particular piece of the hurricane risk analysis framework and presents a novel probabilistic model for storm-surge prediction that is computationally efficient and overcomes such limitations (Contento et al., 2018).

2.3.3 Damage and Loss Models (Step 3)

The hazard scenarios obtained with the models described in Step 2 can be used to obtain predictions of annual damage and loss distributions. In general, the damage estimations are obtained using fragility curves that provide the likely damage states of the structures or infrastructure given the values of the intensity measures describing the wind, rainfall, and storm surge.

Similarly, the loss estimations are obtained using loss-ratio curves. Such curves estimate the losses in the form of a percentage of the initial values of the structures and infrastructure as a function of the intensity measures. These estimations can be obtained for each hurricane scenario. The resulting damage and losses can then be used to derive the corresponding distributions. An example of such procedure can be found in Contento et al. (2017).

The common practice has been to conduct damage and loss assessments (Scawthorn et al., 2006) separately for wind and storm surge with different models and tools (e.g., HAZUS see FEMA, 2009a,b, and CLARA see Johnson et al., 2013). However, this might lead to double counting the damage and losses (since a structure damaged by wind might be also counted as damaged by storm surge). There are only a few recent studies that estimate the damage and losses for the combined effects of wind and storm surge (one example of such studies is Li et al., 2012). Considering the combined effects of wind and storm surge avoids double counting damage and losses. In terms of available software, HAZUS-MH (FEMA, 2012) provides the possibility of performing joint wind-surge damage and loss analyses. To take advantage of the storm-surge probabilistic model developed by Contento et al. (2018) in computing the contribution from the storm surge to the damage and loss estimates, user defined hazard scenarios from Contento et al. (2018) can be used instead of the ones automatically generated by HAZUS using SLOSH and SWAN (Booij et al., 1996).

2.3.4 Development of Mitigation and Adaptation Strategies (Step 4)

The hazard scenarios obtained from Step 2 and the distributions of damage and losses obtained from Step 3 can be used for the development and comparison of mitigation and adaptation strategies (Stewart et al., 2014, see also Chapter 1). Specifically, mitigation strategies would affect the inputs to Step 1, and environmental adaptation strategies would affect the inputs to Steps 2 and 3. The results from Step 3 can be used in decision models for life-cycle risk assessment of structures (e.g., Lee and Ellingwood, 2017; Gardoni et al., 2016). Such decision models guide long-term decisions by incorporating the costs associated to the entire service life of an asset. Incorporating the results from Step 3 in the decision models allows us to consider the effects of mitigation and adaptation strategies in the cost estimates. Finally, the results from Step 3 can inform insurance and financial models, for example, to improve the loss- and uncertainty-dependent components of the insurance premium and catastrophe (CAT) bond pricing (Hofer et al., 2018).

2.4 Hazard Scenario Models: Storm-Surge Modelling

While there are a number of studies on wind field and debris movement during hurricanes and their associated damage, there are only a few studies on storm surge and its associated damage. State-of-the-art storm-surge models can use outputs from wind and pressure field models to generate storm-surge simulations, or observed wind and pressure fields for hindcasts of storm surge (e.g., Houston et al., 1999; Westerink et al., 2008; Bunya et al., 2010). Physics-based models use shallow-water equations (SWEs) to model the hydrodynamics of the storm surge (e.g., Jelesnianski et al., 1992, Westerink et al., 1994, Hubbert and McInnes, 1999, Roland et al., 2009). The most commonly adopted models for storm surge are the ADCIRC model (Westerink et al., 1994) and the SLOSH model (Jelesnianski et al., 1992). The ADCIRC model accurately simulates hurricane storm surge, but also astronomical tides. The model numerically integrates the depth-integrated barotropic SWEs in spherical coordinates over an unstructured grid. The grid has a wide range of element sizes (Westerink et al., 2008) that are chosen to obtain an extremely fine resolution near the coast that becomes coarser and coarser moving towards the deeper ocean, according to the required accuracy. The high-resolution numerical grid used by ADCIRC captures the complex spatial variability of the phenomenon (Dietrich et al., 2011); however, the model is highly computationally demanding. SLOSH was originally developed for real-time forecasting of hurricane storm surges on continental shelves. It solves the SWEs using the finite difference method over a grid (polar, elliptic or hyperbolic) centred on the region of interest (Jarvinen and Lawrence, 1985). The model requires the characteristics of the hurricane to derive a model of the wind field, which drives the storm surge. The main limit of SLOSH is that the accuracy of the storm-surge predictions is highly dependent on the accuracy of the meteorological input and the error in the estimate is about 20% using accurate hurricane predictions (Jelesnianski et al., 1992). Moreover, the model does not account for astronomical tides and wind waves. Lin et al. (2012) used ADCIRC and SLOSH together with grids having different extensions and resolutions, restricting the use of ADCIRC to the area for which the risk assessment requires higher accuracy in the predictions.

Although some of the models available in the literature are accurate, a trade-off between efficiency and accuracy is required when a high number

of simulated scenarios are needed like in the case of probabilistic analysis. In this case, simplified models fitted to available data are a more efficient option. They are developed to approximate the dominant features of a complex model in a computationally efficient way (Asher et al., 2015). Approximate or empirical models can be divided into three main categories (Asher et al., 2015): (i) projection-based methods that project on a reduced subspace the governing equation of the original model; (ii) multifidelity-based methods that either reduce the resolution of the original model or simplify the underlying equations; and (iii) data-driven methods that approximate the original model output with a relation calibrated with inputs and outputs of the same original model. For storm surge, only empirical models (i.e., models that belong to the third category) can be found in the literature. They are calibrated using inputs and outputs obtained by a limited number of physics-based simulations of storm-surge scenarios. As outputs, they provide estimates of the storm surge at predefined locations (points) in the domain of the model, which are the locations of the observations used for the model calibration (Irish et al., 2008; Jia and Taflanidis, 2013; Kim et al., 2015; Jia et al., 2016). While computationally efficient, such empirical models generally lack physical meaning in their functional form.

Irish et al. (2008) developed an empirical model for storm-surge height as a function of the central pressure, radius of maximum wind speed, and forward velocity of the hurricane. The model was calibrated using ADCIRC simulations. Such simulations used synthetic hurricanes to drive the storm surge. The sustained near-surface winds used in the simulations were estimated using a coupled hurricane vortex-planetary boundary layer model (Thompson and Cardone, 1996). This empirical model presented a simplified formulation whose aim was to show the dependence of the storm surge on the size of the hurricane but not to obtain accurate estimates of storm surge. Jia et al. (2016) developed a Kriging model to predict storm surge over an extended coastal region. To improve the computational efficiency of the Kriging model, they integrated the principal component analysis (Jolliffe, 2002) in their formulation. The results presented in Jia et al. (2016) showed that their empirical model is capable of providing accurate predictions of both storm surge and wave height. However, the model was subject to a computationally demanding calibration that required 400 combined ADCIRC and SWAN simulations (Dietrich et al., 2011). Also, artificial neural networks (ANNs) have been used for storm-surge prediction. Kim et al. (2015) developed a time-dependent empirical model for storm surge

using an ANN trained with high-fidelity simulations of two historical hurricanes. While ANNs are a good option for problems that are highly nonlinear or have a large amount of data, they are usually best suited for deterministic applications and may not significantly reduce the computational expenses. In general, common limitations of the empirical models on storm surge available in the literature are that: (i) they cannot include in the calibration data recorded or computed at different locations between storms (as a result, it is typically difficult to include both historical data and data from simulations because historical data are typically sparser than simulation data); and (ii) they can provide estimates of storm surge only in the points used for model calibration (as a result, a separate interpolation among the predictions is needed to estimate the storm-surge height over the region of interest).

The probabilistic model presented in Contento et al. (2018), and discussed in the next sections, can be a valid alternative for probabilistic analyses of storm surge. In addition, the model in Contento et al. (2018) is also able to capture the effects of climate change. The model combines a logistic regression model and a nonstationary random field. The logistic regression model estimates the probability of one location being wet (i.e., flooded), as a function of physical regressors affecting the storm surge. The random field estimates the distribution of the surge height over the wet locations. The random field is developed using the improved latent space approach (ILSA) proposed in Xu and Gardoni (2018). Specifically, the ILSA-based random field considers physical regressors as latent dimensions in addition to the spatial dimensions, and models the mean, variance, and spatial correlation of the storm surge as functions of such regressors. Therefore, such a model is particularly suited to model the nonstationarity in the storm-surge distribution on the basis of physical principles.

Differently from the empirical models available in the literature, the probabilistic model presented in Contento et al. (2018) can be trained using both results from historical records and high-fidelity simulations, and can provide predictions at locations different from those of the observations used for the model calibration. In addition, the model calibration is computationally efficient because it requires a limited amount of data for calibration to provide accurate predictions. The consequent advantage is that comparative analyses on the effects of climate change for different climate change scenarios can be performed training the model with results from a limited amount of simulations for each scenario.

2.4.1 Physics of the Storm Surge and Storm-Surge Data

The intense circular motion of the wind around the eye of a hurricane that occurs on the surface of the ocean generates a vertical circular motion in the oceanic waters (Resio and Westerink, 2008). As the storm approaches the coast, and the depth of the ocean decreases, the bottom of the ocean disturbs the vertical motion generating a storm surge, an anomalous rise of water above the expected astronomical tide. In the low-lying coastal areas, where the motion of the water is not prevented by natural or artificial barriers the water penetrates inland. Two different groups of factors, the geomorphological features of the landing site and the characteristics of the hurricane, influence the storm-surge intensity. For a given location, among the characteristics of the landing site, the one that is mentioned in the literature as having the highest impact on the storm-surge height is the mean altitude of the area affected by the storm surge. The hurricane characteristics that affect the storm surge are those related to the intensity of the hurricane (i.e., the wind speed, the central pressure, and the hurricane forward speed), to its track (i.e., the landfall location and the angle of approach to the coast), as well as the size of the storm.

To develop a probabilistic model for storm-surge predictions, it is fundamental to take into account the characteristics mentioned above. In the proposed model, this is done by introducing explanatory functions described in Section 2.4.2. To define the explanatory functions, the vector of storm-surge heights, $\mathbf{y}$, at different locations in the region of interest has to be provided along with the vector of corresponding characteristics of the locations, $\mathbf{x}$, and the vector of hurricane characteristics, $\mathbf{s}$. The location characteristics considered in the model are the longitude, x_{1j_i}, latitude, x_{2j_i}, and altitude, x_{3j_i}, of each measurement location $j_i = (1, \ldots, m_i)$, for each hurricane $i = (1, \ldots, n)$. The hurricane characteristics considered are the longitude and latitude of the hurricane landing point, s_{1i} and s_{2i}; the heading angle of the hurricane at landing, s_{3i}; the central pressure (pressure in the eye of the hurricane), s_{4i}; the forward velocity, s_{5i}; and the radius of maximum wind speed, s_{6i}. Fig. 2.1 shows some of the characteristics included in $\mathbf{s}$ and $\mathbf{x}$. Table 2.1 shows schematically what data are needed for the model calibration and how they are organised. In the table, the subscript o stands for 'observation' to clarify that the quantities are data needed to calibrate the model.

The storm-surge data used to show the capabilities of the model discussed in this chapter come from simulations performed by Kendra et al. (2017). The simulations are performed coupling hurricane wind/

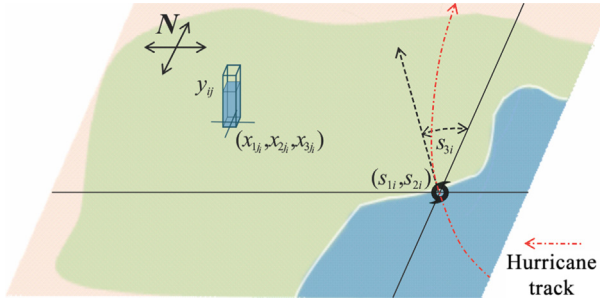

Fig. 2.1 Graphic representation of location and hurricane characteristics.

Table 2.1 Format of the Storm-Surge Observations

Hurricane event	Storm-surge observations y_o	Location characteristics x_o			Hurricane characteristics s_o					
		x_{o1}	x_{o2}	x_{o3}	s_{o1}	s_{o2}	s_{o3}	s_{o4}	s_{o5}	s_{o6}
1	y_{o11}	x_{o11_1}	x_{o21_1}	x_{o31_1}	s_{o11}	s_{o21}	s_{o31}	s_{o41}	s_{o51}	s_{o61}
	y_{o1j}	x_{o1j_1}	x_{o2j_1}	x_{o3j_1}						
	y_{o1m_1}	x_{o1m_1}	x_{o2m_1}	x_{o3m_1}						
i	y_{oi1}	x_{o11_i}	x_{o21_i}	x_{o31_i}	s_{o1i}	s_{o2i}	s_{o3i}	s_{o4i}	s_{o5i}	s_{o6i}
	y_{oij}	x_{o1j_i}	x_{o2j_i}	x_{o3j_i}						
	y_{oim_i}	x_{o1m_i}	x_{o2m_i}	x_{o3m_i}						
n	y_{on1}	x_{o11_n}	x_{o21_i}	x_{o31_n}	s_{o1n}	s_{o2n}	s_{o3n}	s_{o4n}	s_{o5n}	s_{o6n}
	y_{onj}	x_{o1j_n}	x_{o2j_n}	x_{o3j_n}						
	y_{onm_n}	x_{o1m_n}	x_{o2m_n}	x_{o3m_n}						

precipitation, hydrologic, hydrodynamic, and wave models. For every hurricane scenario used as input, a simulation provides the corresponding storm-surge scenario. The dependence of the storm-surge scenarios on the effects of climate change is captured by considering the effects of climate change on the hurricane scenarios. For each hurricane both track and characteristics are derived under the worst-case climate scenario presented in the IPCC AR5 report (IPCC, 2013). Such scenario is the 8.5 Representative Concentration Pathway (RCP 8.5), which assumes a radiative forcing level of 8.5 W/m^2 in 2100.

Kendra et al. (2017) generated 238 storm-surge scenarios that include 1200 data over the stretch of the Tar and Pamlico River between the cities of Greenville and Washington in North Carolina. To show that the chosen approach does not require a high number of observations to produce accurate results, from the available 238 sets of observations, we randomly select

25 sets of observations for the model selection and calibration, where a set refers to a specific hurricane and associated storm-surge scenario.

Although the data refer to a specific time and region (in 2100 and the Pamlico River area), the probabilistic model presented by Contento et al. (2018) could be used to estimate the quantities of interest also for different times and regions as long as the values of **x** and **s** are within the range of the values used to calibrate the models. Since **x** and **s** might miss some location characteristics and/or hurricane characteristics, the model could also be retrained or updated by Bayesian updating with new data for a specific time and region when available. For example, the model could be updated with the results of new simulations based on new hurricane scenarios (possibly reflecting better predictions on the effects of climate change).

For the model calibration and validation, three groups of observations are created. The first group (Group A) is used for the model selection and calibration. Group B is used for the model validation considering hurricane characteristics used in the model calibration but considering different locations. Group C is used for the model validation considering locations used in the model calibration but considering different hurricane characteristics.

Specifically, Group A contains observations at 60 locations that are the same for each of the 25 scenarios, for a total of 1500 observations. Among these observations, 70% are used for model selection and calibration. The model selection and calibration is repeated resampling the 70% of the observations to check consistency in the results (i.e., that the results do not depend on the selected data). Group B contains observations at 20 new locations that are again the same for each of the 25 scenarios, for a total of 500 observations. Group C contains observations at the same 60 locations considered for the observation of Group A, but coming from four additional scenarios. To avoid extrapolation in the prediction of the storm-surge height, these four scenarios are selected so that the characteristics of the hurricanes falls within the ranges of the characteristics of the hurricanes used for model calibration. Fig. 2.2 shows the locations of the observations in Groups A, B, and C.

2.4.2 Probabilistic Model for Storm Surge

The probabilistic model presented by Contento et al. (2018) combines two different models: a logistic regression model and a nonstationary random field. The logistic regression model predicts if the single location is wet or dry. While, the random field based on the ILSA approach predicts the

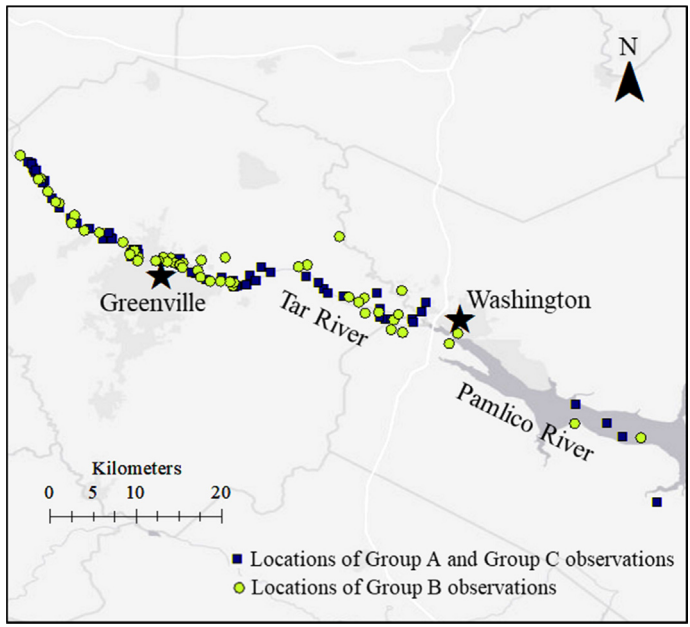

Fig. 2.2 Area of the locations of the storm-surge observations.

storm-surge height, y_{ij}, for the wet locations ($y_{ij} > 0$). Contrary to other models in the literature, the ILSA-based random field model allows for the combined use of observations coming from historical records and high-fidelity model simulations even if they are at different locations. Both the logistic regression model and the ILSA-based random field use explanatory functions to capture the underlying physics of the phenomena. The explanatory functions are selected from an initial set of candidates. Such explanatory functions are combinations of the location and hurricane characteristics **x** and **s**. The candidate explanatory functions are either taken from the literature (Irish et al., 2008; Jia and Taflanidis, 2013) or considered because of their physical meaning. Table 2.2 presents the complete list of the candidate explanatory functions h'_{qij}. Each functions is then standardised to be dimensionless as follows $h_{qij} = [h'_{qij} - E(h'_{qij})]/\mathrm{Var}(h'_{qij})$ where $E(h'_{qij})$ is the sample mean of h'_{qij} and $\mathrm{Var}(h'_{qij})$ is the sample variance of h'_{qij} obtained considering all i and j. Fig. 2.3 shows the physical meaning of the h'_{qij} with geographic meaning (i.e., directions, locations, and distances).

Since locations with altitude $x_{3j_i} \leq 0$ (i.e., locations below the sea level) are more likely to be wet, both the logistic regression and the random field model are calibrated and validated separately for locations with $x_{3j_i} > 0$ and

Table 2.2 Explanatory Functions That Capture the Geomorphological Features of the Landing Site and the Characteristics of the Hurricane

Function	Description
$h'_{0ij}=1$	Intercept
$h'_{1ij}=g(x_{1j_i}, s_{1i}, s_{2i})$	Longitudinal distance between observation location and landing point
$h'_{2ij}=g(x_{2j_i}, s_{1i}, s_{2i})$	Latitudinal distance between observation location and landing point
$h'_{3ij}=x_{3j_i}$	Altitude of the observation location
$h'_{4ij}=g(x_{1j_i}, x_{2j_i}, s_{1i}, s_{2i})$	Distance between observation location and landing point
$h'_{5ij}=s_{1i}$	Longitude of the landing point
$h'_{6ij}=s_{2i}$	Latitude of the landing point
$h'_{7ij}=s_{3i}$	Heading angle of the hurricane at landing
$h'_{8ij}=s_{4i}$	Central pressure
$h'_{9ij}=s_{5i}$	Forward velocity
$h'_{10ij}=s_{6i}$	Radius of maximum wind speed
$h'_{11ij}=\cos[g(x_{1j_i}, x_{2j_i}, s_{1i}, s_{2i})]$	Cosine of the angular distance between the direction of the heading angle and the direction connecting the observation point to the landing point (cosine of the angle h^{*}_{11ij} in Fig. 2.3)
$h'_{12ij}=s^2_{4i}$	Second power of the central pressure
$h'_{13ij}=s_{4i}\cdot s_{6i}$	Cross product of central pressure and radius of maximum wind speed
$h'_{14ij}=s_{4i}/s_{6i}$	Ratio of central pressure and radius of maximum wind speed

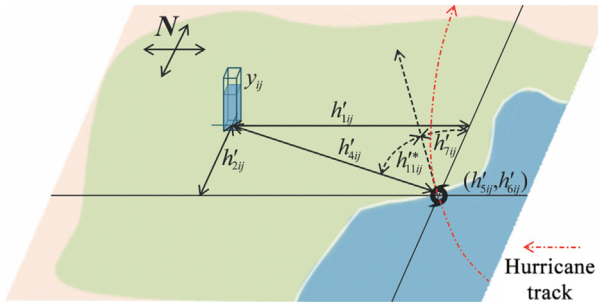

Fig. 2.3 Graphic representation of selected explanatory functions.

$x_{3j_i} \leq 0$. In order to do so, the observations in Groups A–C are divided into two groups. Group 1 contains the observations with $x_{3j_i} > 0$, and Group 2 contains the observations with $x_{3j_i} \leq 0$. The model selection is done without considering this distinction.

2.4.2.1 Logistic Regression Model

First, the logistic regression model is used to estimate the probability p_{ij} that a given location j is wet for a certain hurricane i. The model is written as:

$$p_{ij}\left(\mathbf{x}_{j_i}, \mathbf{s}_i, \boldsymbol{\theta}_l\right) = \frac{\exp\left[\boldsymbol{\theta}_l^{\mathrm{T}} \cdot \mathbf{h}_{ij}^{*}\left(\mathbf{x}_{j_i}, \mathbf{s}_i\right)\right]}{1 + \exp\left[\boldsymbol{\theta}_l^{\mathrm{T}} \cdot \mathbf{h}_{ij}^{*}\left(\mathbf{x}_{j_i}, \mathbf{s}_i\right)\right]} \tag{2.1}$$

where $\boldsymbol{\theta}_l$ is the vector of model parameters, and $\mathbf{h}_{ij}^{*}(\mathbf{x}_{j_i}, \mathbf{s}_i)$ is the vector of the powers of the h_{qij}, from the first to the fourth order. Starting from the full vector, Contento et al. (2018) use a selection process to remove the explanatory functions that are statistically insignificant. The selection process has two steps. The first step uses the Akaike information criterion (AIC) (Akaike, 1974) for a preliminary selection. The second step uses a cross-validation technique to make the final selection. In this second step, the selection process randomly divides the observations used for model selection (Group A) into a calibration set (80% of the observations) and a selection set (20% of the observations). Then, it calibrates all of the competing models using the calibration set, and generates several test sets through resampling of the selection set. The cross-validation technique selects a reduced number of candidates by comparing the models' prediction errors (the total number of wrong predictions for the test sets). Specifically, for each candidate model, the selection process computes the mean value and the 95% confidence interval of the model error. Then, the process chooses as final candidates the models whose 95% confidence interval includes the lowest mean value. Among these candidate models, the selection process finally selects the model that has the least number of explanatory functions. The selected model is then recalibrated using all the data in Group A. Fig. 2.4 shows the selection process for the 11 candidate models with the lowest AIC. For each of the 11 models showed in the example, the dot represents the mean value of the model error while the bar shows the 95% confidence interval. Among the models with a low prediction error, only Models 5–8 have a 95% confidence interval that contains the lowest mean prediction error that is the one of Model 5. Since Model 5 has fewer explanatory functions than any of the Models 5–8, the final model is Model 5. For the selected model, the model parameters, $\boldsymbol{\theta}_l$, are estimated using a Bayesian approach (Gardoni et al., 2002). The form of Model 5 along with the statistics of the model parameters can be found in Contento et al. (2018). Once the posterior distribution of the model parameters, $f''(\boldsymbol{\theta}_l)$, is found, a predictive

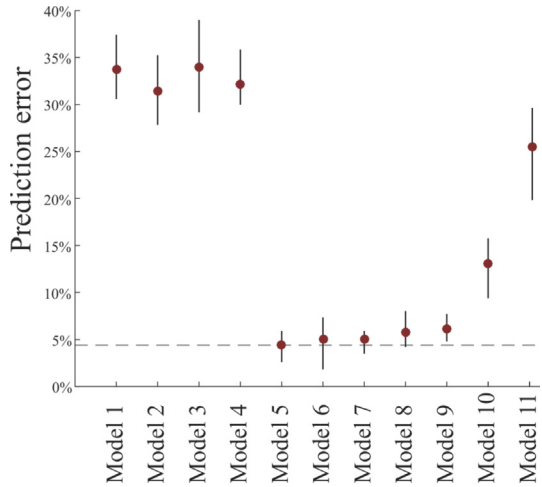

Fig. 2.4 Mean values (*dots*) and 95% confidence intervals (*bars*) of the prediction error for the different models.

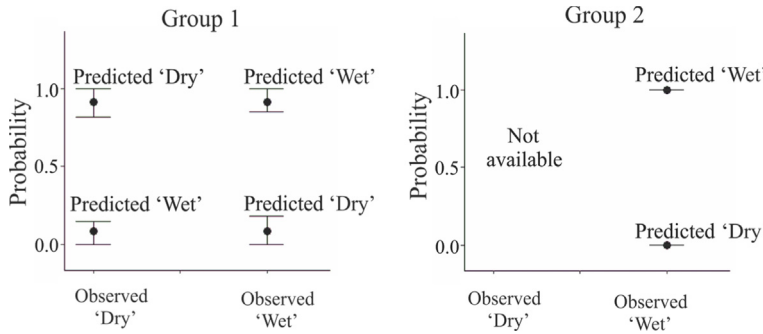

Fig. 2.5 Predicted probabilities of dry and wet observations.

estimate, $\widetilde{p}_{ij}\left(\mathbf{x}_{ji}, \mathbf{s}_i\right)$, of the probability of the location j being wet is obtained following Gardoni et al. (2002).

Fig. 2.5 shows the comparison between observations and predictions for the data used in the model calibration (80% of Group A) divided into Groups 1 and 2 as described earlier. In each of the two graphs, the dots represent the mean probabilities for wet and dry locations to be predicted as wet or dry. The bars are the one standard deviation confidence intervals. Since all the observation in Group 2 are wet, the model predicts that these locations are wet with probability close to 1 and confidence intervals close to 0 (the small difference from 1 and 0 is due to the numerical approximations in finding $\boldsymbol{\theta}_l$).

2.4.2.2 Random Field Model

A nonstationary spatial random field is used to estimate the storm-surge height for the wet locations. The general formulation of a nonstationary spatial random field can be found in, for example, Schmidt et al. (2011). Generally, a random field is composed by three terms: a mean structure of the field; a zero-mean nonstationary random field; and a white noise. The mean structure describes the mean value of the quantity of interest as it varies spatially. The zero-mean nonstationary random field captures the nonstationary covariance. The white noise captures the micro-scale uncertainty. The mean structure is typically a deterministic function ideally constructed based on the underlying physics of the phenomenon. The covariance generally is constructed using a parametric function. Finally, the white noise is typically modelled with an additive zero mean normal random variables with unknown standard deviation.

The random field used in Contento et al. (2018) is based on the ILSA proposed by Xu and Gardoni (2018). The random field is modelled as a function of explanatory functions, $\mathbf{h}_{ij}(\mathbf{x}_{j_i}, \mathbf{s}_i)$, which are considered as latent dimensions of the random field. For purpose of normalisation, the random field model is developed for the natural logarithm of the storm-surge heights, $\mathbf{z} = \ln(\mathbf{y})$. The random field is written as:

$$z_{ij}\left(\mathbf{x}_{j_i}, \mathbf{s}_i, \boldsymbol{\theta}_{IL}\right) = m\left(\mathbf{x}_{j_i}, \mathbf{s}_i, \boldsymbol{\theta}_m\right) + \nu\left(\mathbf{x}_{j_i}, \mathbf{s}_i, \boldsymbol{\theta}_\Sigma, \boldsymbol{\theta}_\sigma\right) + \sigma\varepsilon\left(\mathbf{x}_{j_i}\right) \tag{2.2}$$

where the mean field, $m(\mathbf{x}_{j_i}, \mathbf{s}_i, \boldsymbol{\theta}_m)$, the zero mean correlated field, $\nu(\mathbf{x}_{j_i}, \mathbf{s}_i, \boldsymbol{\theta}_\Sigma, \boldsymbol{\theta}_\sigma)$, and the white noise $\sigma\varepsilon(\mathbf{x}_{j_i})$ contain model parameters, $\boldsymbol{\theta}_{IL} = (\boldsymbol{\theta}_m, \boldsymbol{\theta}_\Sigma, \boldsymbol{\theta}_\sigma, \sigma)$, that are calibrated using the data described in Section 2.4.1. The mean field is a linear combination of the explanatory functions:

$$m\left(\mathbf{x}_{j_i}, \mathbf{s}_i, \boldsymbol{\theta}_m\right) = \sum\nolimits_k \theta_{mk} h_k\left(\mathbf{x}_{j_i}, \mathbf{s}_i\right) \tag{2.3}$$

The variances and spatial correlations in the zero-mean nonstationary random field are modelled as functions of the Euclidian distance, the differences between explanatory functions at two locations, and unknown model parameters. The elements of the covariance matrix given by $\nu(\mathbf{x}_{j_i}, \mathbf{s}_i, \boldsymbol{\theta}_\Sigma, \boldsymbol{\theta}_\sigma)$ and the white noise can be written as:

$$\begin{aligned}\left[\boldsymbol{\Sigma}_{\mathbf{zz}}(\mathbf{x}, \mathbf{s}, \boldsymbol{\theta}_\Sigma, \boldsymbol{\theta}_\sigma, \sigma)\right]_{rs} &= \left[\boldsymbol{\Sigma}_{\mathbf{vv}}(\mathbf{x}, \mathbf{s}, \boldsymbol{\theta}_\Sigma, \boldsymbol{\theta}_\sigma)\right]_{rs} + \sigma^2 \cdot 1_{\{r=s\}} \\ &= \sigma_\nu^2(\mathbf{x}, \mathbf{s}, \boldsymbol{\theta}_\sigma) \cdot \exp\left[-Q_{rs}(\mathbf{x}, \mathbf{s}, \boldsymbol{\theta}_\Sigma)\right] + \sigma^2 \cdot 1_{\{r=s\}}\end{aligned} \tag{2.4}$$

where $\sigma_v(\mathbf{x}, \mathbf{s}, \boldsymbol{\theta}_\sigma)$ is the standard deviation, $Q_{rs}(\mathbf{x}, \mathbf{s}, \boldsymbol{\theta}_\Sigma)$ is the generalized distance in the correlation function, and σ^2 is the variance of the white noise, $\mathbf{x} = [\mathbf{x}_{j_i}]\ \forall i, j$, and $\mathbf{s} = [\mathbf{s}_i]\ \forall i$. Details for deriving $\sigma_v(\mathbf{x}, \mathbf{s}, \boldsymbol{\theta}_\sigma)$ and $Q_{rs}(\mathbf{x}, \mathbf{s}, \boldsymbol{\theta}_\Sigma)$ can be found in Xu and Gardoni (2018).

For the ILSA-based random field, the model selection starts from the full vector of the explanatory functions, $\mathbf{h}_{ij}(\mathbf{x}_{j_i}, \mathbf{s}_i)$. To avoid underestimating the storm-surge height, Contento et al. (2018) used only the wet observations in Group A for the model selection of the random field. The model calibration and selection is done as for the logistic regression.

In this case, all the 15 explanatory functions shown in Table 2.2 are retained in the selected model. After the parameter estimation, a predictive joint distribution of the natural logarithms of the storm-surge heights $\tilde{\mathbf{z}}(\mathbf{x}, \mathbf{s})$ is derived using the posterior distribution of $\boldsymbol{\theta}_{IL}, f''(\boldsymbol{\theta}_{IL})$. The median predictions of the storm-surge heights $\tilde{\mathbf{y}}(\mathbf{x}, \mathbf{s})$ and their confidence intervals are consequently derived from $\tilde{\mathbf{z}}(\mathbf{x}, \mathbf{s})$. The form of the selected model, along with the statistics of the model parameters, and an exhaustive explanation on the derivation of $\tilde{\mathbf{y}}(\mathbf{x}, \mathbf{s})$ can be found in Contento et al. (2018).

Fig. 2.6 show the results of the fitting obtained for the observations in Groups 1 and 2. The dots in Fig. 2.6 are the predicted heights versus the actual observed heights, while the diagonal lines are the 1:1 lines that represent perfect predictions. The predictions for both Groups 1 and 2 are unbiased.

2.4.3 Water Depth Predictions

For each set of location and hurricane characteristics, the model provides predictions in terms of the probability of having a wet location, $\tilde{p}_{ij}(\mathbf{x}_{j_i}, \mathbf{s}_i)$, and the marginal distribution of the storm-surge height

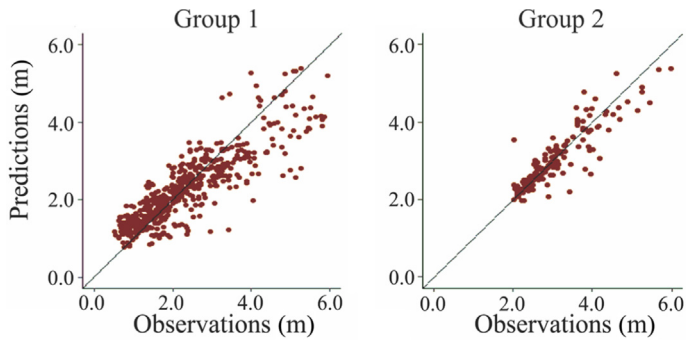

Fig. 2.6 Fitting of the training data for the random field model y_{ij}.

$\widetilde{\gamma}_{ij}(\mathbf{x}_{j_i}, \mathbf{s}_i)$. Since the distribution of the storm-surge height refers to the mean sea level, alone it is not an exhaustive piece of information and, at the same time, does not convey an intuitive representation of the flooding risk. To solve this issue, an option is to provide results in terms of water depth, $k_{ij}(\mathbf{x}_{j_i}, \mathbf{s}_i)$, at the site. The prediction for the water depth can be obtained by subtracting the altitude of the prediction location x_{3j_i} from the prediction of the storm-surge height as:

$$\widetilde{k}_{ij}(\mathbf{x}_{j_i}, \mathbf{s}_i) = \widetilde{\gamma}_{ij}(\mathbf{x}_{j_i}, \mathbf{s}_i) - x_{3j_i} \tag{2.5}$$

Consequently, with this transformation, a prediction is completely defined by the two values $\left[\widetilde{p}_{ij}(\mathbf{x}_{j_i}, \mathbf{s}_i), \widetilde{k}_{ij}(\mathbf{x}_{j_i}, \mathbf{s}_i)\right]$.

We can now look at the accuracy of the calibrated models in predicting the likelihood that a location is wet and the corresponding water depth (if a location is wet) for different locations than then ones used in the models calibration (but for the same hurricanes), and for different hurricanes. The first set of predictions is made considering the observations in Group B (described in Section 2.4.1). In this case, the predictions are made for hurricane characteristics taken from the initial set of 25 hurricanes chosen for the model calibration, but for locations different from those used to develop the model. The second set of predictions is made considering the observations in Group C. In this second case, the hurricane characteristics are different from those in the data used for the model calibration.

2.4.3.1 Predictions at Different Locations

Fig. 2.7 shows the results for different locations (but the same hurricanes). The dots show the median predictions versus the observations, while the bars are the corresponding one standard deviation confidence intervals. The diagonal lines represent the perfect correspondence between the predictions and observations. For each prediction, the lower is the probability that the location is wet, the dimmer is the colour of the dot and corresponding bar. In this way, it is possible to combine the information from the logistic regression model and the random field.

Fig. 2.7 shows the predictions corresponding to the data in Groups 1 and 2. In general, the values of the observations and predictions for the locations in Group 2 are higher than those in Group 1. The reason is that these locations are those on the riverbed, and the initial water height is summed to the storm surge when considering the water depth (the altitude is negative).

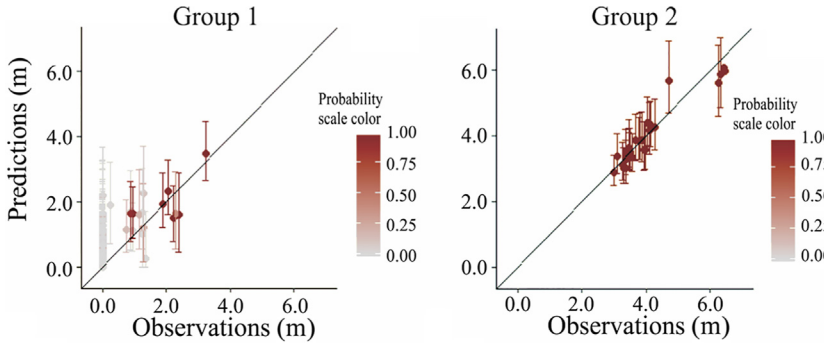

Fig. 2.7 Predictions of water depth k_{ij} due to hurricanes used to calibrate the model (different locations).

In Fig. 2.7, the darker colour of the markers show that generally for Group 1 the model predicts higher values of the water depth with higher confidence. This tendency of the model means that the locations with higher values of water depth, for which the risk of damage is higher, are more likely correctly identified. Fig. 2.7 also shows that the locations of the observations in Group 2 are all correctly predicted as wet (consistently with the results shown in Fig. 2.5). The mean values of the ILSA-based random field predictions are generally more accurate (closer to the 1:1 line) than those for the locations in Group 1.

2.4.3.2 Predictions for Different Hurricanes

The predictions for hurricane scenarios not used in the model calibration are made using the four hurricanes with characteristics shown in Table 2.3.

Figs. 2.8 and 2.9 show the predictions of the water depth obtained for the four additional hurricane scenarios. The meaning of markers, bars, and colours is the same explained in Fig. 2.7.

Generally, we can make similar observations as those made for Fig. 2.7. The highest values of water depth are predicted with good accuracy and, at the same time, the related locations have a high probability of being wet. The accuracy in the prediction increases for the observations belonging to Group 2. The predictions presented in Section 2.4.3 do not aim to exemplify an exhaustive study on the effects of climate change on storm surge but they show that the probabilistic model presented in Contento et al. (2018) is a suitable tool that can be used for probabilistic analyses on storm surge considering or not the effects of climate change.

Table 2.3 Hurricane Characteristics

	Hurricane characteristics					
Hurricane	s_1 (°lon)	s_2 (°lat)	s_3 (rad)	s_4 (hpa)	s_5 (m/s)	s_6 (km)
1	−76.162	34.856	5.16	989.81	5.02	52.80
2	−75.518	35.112	5.75	986.83	3.13	47.77
3	−75.736	35.142	5.22	988.57	5.22	38.85
4	−75.695	35.156	5.16	994.82	5.94	36.29

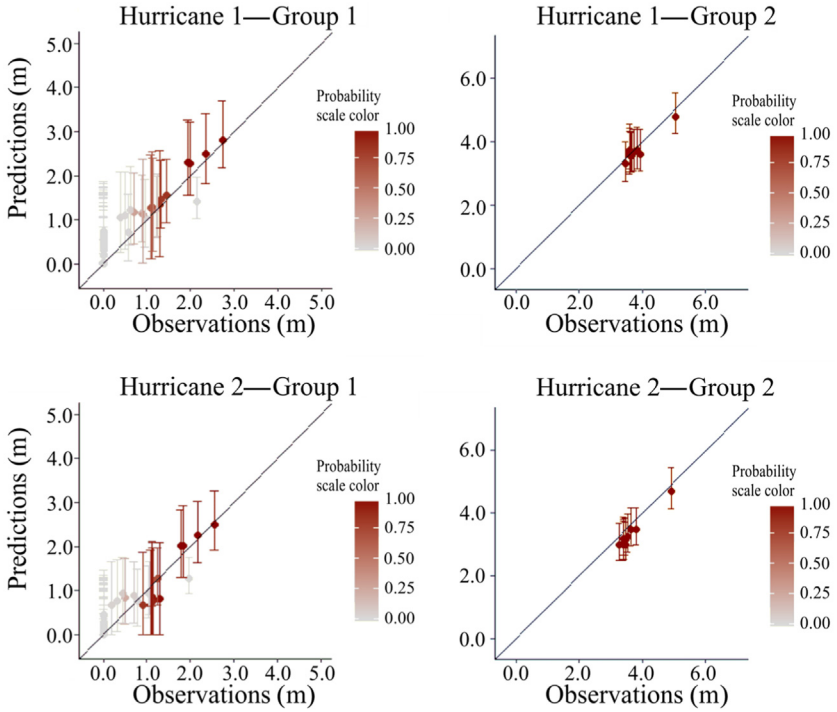

Fig. 2.8 Predictions of water depth k_{ij} for different hurricanes characteristics (Hurricane 1 and 2).

2.5 Development of Mitigation and Adaptation Strategies

This section describes in more detail the use of the results from the storm-surge model (described in Section 2.4 and part of Step 2 of the general framework for hurricane risk analysis) and of the results from the loss estimates from Step 3 of the framework.

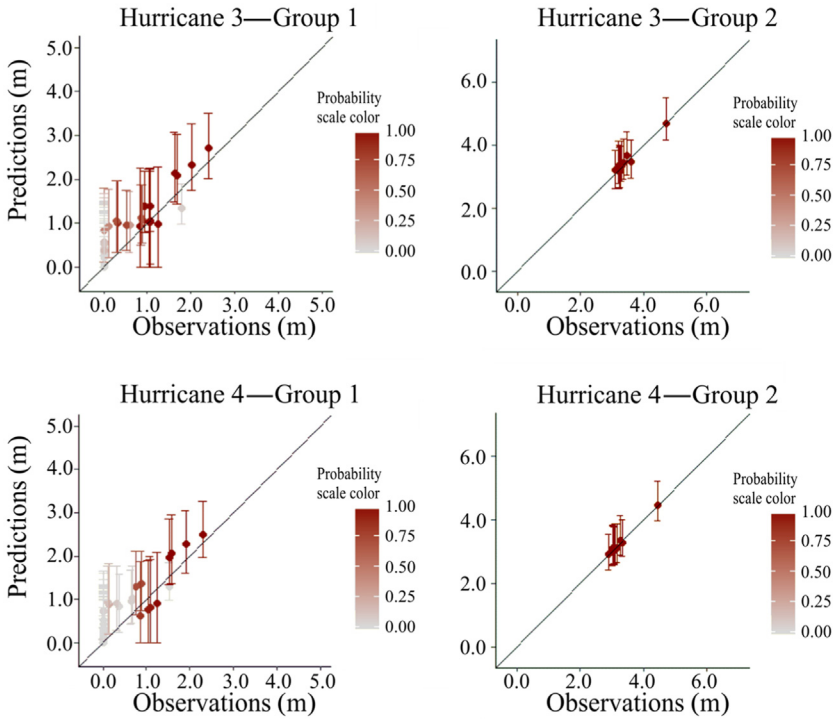

Fig. 2.9 Predictions of water depth k_{ij} for different hurricanes characteristics (Hurricane 3 and 4).

2.5.1 Use of Storm-Surge Predictions

Storm-surge predictions can be used in the form of hazard maps that provide information (e.g., the base flood elevation) for the choice of mitigation and adaptation strategies. At the level of the built or modified natural environment, hazard maps can be used to guide in the development of adaptation strategies. Such strategies could be both interventions on structural elements (e.g., elevating buildings on piles, installing breakaway walls, improving pile foundations, installing opening in foundation walls) and on nonstructural elements (e.g., elevating equipment, constructing flood-resistant equipment enclosures) (FEMA, 2005). The development of accurate hazard maps that account for the effects of climate change play an important role in defining the specific design characteristics of such adaptation strategies (i.e., the height of the elevated floors, and the characteristics of breakaway walls).

At the community level, hazard maps can inform on the effectiveness of mitigation strategies in terms of their ability to reduce the effects of climate change on the characteristics of the hazard. Hazard maps can also be used as a

planning tool for environmental and human adaptation strategies. For the environmental adaptation strategies, hazard maps may help identify the most effective locations and characteristics of structures such as seawalls, levees and storm-surge barriers (FEMA, 2005), or green infrastructure such as wetland. For the human adaptation strategies, hazard maps may help establish evacuation routes, define high-risk areas where development should be avoided by enforcing specific zoning policies, and define the most suitable areas for relocation that could be a successful way to adapt to both sea-level rise and storm surge (Olshansky, 2018).

2.5.2 Use of Damage and Loss Estimations

Damage and loss distributions obtained from the third step of the framework can be used for the comparison of mitigation and adaptation strategies through the evaluation of their cost-effectiveness (Bjarnadottir et al., 2011), in decision models for life-cycle risk assessment of structures and infrastructure (Lee and Ellingwood, 2017; Gardoni et al., 2016), and in financial models used to device strategies to edge the risks (Grace et al., 2005; Jaffee et al., 2010; Hofer et al., 2018). In this section, we focus specifically on the use of the damage and loss estimations in financial models and specifically on insurance premium and CAT bond pricing. Insurance premium and CAT bond pricing, although different, are both directly affected by the risk associated to the policy (Grace et al., 2005) and the uncertainties in their estimation (Hofer et al., 2018). Modern pricing techniques can be used to devise effective risk hedging opportunities. To be effective, such techniques need accurate loss estimations that account for the underlying uncertainties.

The pricing of insurance premiums depends on several factors such as the required deductible, the desired coverage amount, and the risk associated to the policy. The deductible and the coverage amount are set a priori. On the other hand, the risk associated to the policy is more difficult to define because it depends on several aspects such as the kind of hazard and the characteristics of the insured property (e.g., type and location). Different insurance companies adopt different formulations for pricing the premiums. Using a generic formulation, Contento et al. (2017) compared the expected hurricane insurance premiums considering the present climate conditions as well as the RCP 8.5 climate change scenario. The results suggested an increase in the premium due to the effects of climate change that ranges from 5% to 20% depending from the type of building to be insured. There are several strategies to avoid excessive increases in premium. The most

common strategies consist in acting directly on the premium by adding or increasing the deductible, transferring part of the insurance exposure to reinsurance companies, or transferring part of the insurance risks to the capital market using insurance-linked securities like CAT bonds (Ou Yang, 2010; Hofer et al., 2018).

CAT bonds are risk-linked securities that transfer a specified set of risks from a sponsor to investors. CAT bonds are structured as coupon-paying bonds with default linked to the occurrence of a trigger event. There are different types of trigger events for hurricane CAT bonds. Some of them are related to the occurrence and characteristics of the individual event (i.e., the occurrence of a hurricane with intensity higher than a predefined threshold), others are related to the consequences of the event (i.e., the exceedance of a set amount of losses for a single insurance or in a specific area of interest). In both cases the trigger event may be affected by the effects of climate change. For the first type of trigger events, the effects would be captured by the results of Steps 1 and 2. For the second type, the effects would be captured by the results of Step 3.

2.6 Summary

The terms 'mitigation' and 'adaptation' strategies are typically used with different meanings in the contexts of natural hazards and climate change. The chapter started by providing clear definitions of 'mitigation' and 'adaptation' strategies, and proposing a consistent use of these terms with dealing with natural hazards affected by climate change.

Then, the chapter presented a general framework for hurricane risk analysis. The framework has four steps: the modelling of the hurricane activity, the modelling of the hazard scenarios, the modelling of damage and losses, and the development of mitigation and adaptation strategies. This chapter presented a probabilistic model for storm-surge predictions that can be used in the second step of the framework. The chapter also showed the possible use of the information obtained by a risk analysis in the development of mitigation and adaptation strategies.

The probabilistic model for storm-surge predictions combines a logistic regression model and random field. The logistic regression model estimates the probability that a location is wet. The random field estimates the corresponding distribution of water depth. The main advantages of this model compared to those available in the literature are its computational

efficiency, the possibility to be calibrated with data coming from both high-fidelity simulations and historical records, and its ability to provide predictions at locations different from those for which the model was calibrated. The chapter showed examples of predictions that have been obtained calibrating the model with data from high-fidelity model simulations. Such simulations were performed assuming the effects of the climate change scenario described by the RCP 8.5.

The last part of the chapter showed the possible uses of hazard maps (obtained in the second step of the framework), and of damage and loss estimations (obtained in the third step). Hazard maps are an important instrument for the choice and design of mitigation and adaptation strategies both at the level of the built or modified natural environment and at the community level. Damage and loss estimates can be used for the comparison of mitigation and adaptation strategies, in decision models for life-cycle risk assessment of structures and infrastructure, and in financial models. Specifically considering financial models, the chapter showed how the results of the risk analysis can inform the insurance premiums and the pricing of CAT bonds.

2.7 Potential Design and Practice Evolutions

The use of risk analyses could help the design process both at the level of the built or modified environment and the community. At the level of the built or modified environment level, it could help define specific design characteristics. For example, hazard maps providing the base flood elevation derived based on a selected climate change scenario could be adopted in the common practice. At the community level, risk analyses could help in land planning processes. However, current state-of-the-art tools (i.e., software) for hurricane risk analyses are largely research tools rather than design tools. The development of new design-oriented tools could help the evolution of the engineering practice.

2.8 Open Research Questions

This chapter shows a framework for hurricane risk analysis, as well as some of the most advanced theoretical models that can be used as part of such framework. However, there are several aspects within such framework that could be improved. One aspect is that the predictions of damages and losses

carry a high uncertainty deriving from the choice of the climate change scenario. A higher control of greenhouse gasses emissions on one side and the improvement of climatological models on the other could reduce the uncertainty in the choice of the scenario to adopt and in the projections for a given scenario. The reduction of the uncertainty in the hazard description would consequently be reflected in the uncertainty in the damage and loss estimations. Another aspect is related to the models available in the literature and consequently included in the available software. In most of the cases, the dependence of the models in Steps 1 and 2 on climate change is restricted to the use of projections of SSTs. The reason is that changes in SSTs are projected with higher confidence than changes in most of the other climatological variables. Adding the dependence of the models on other climatological variables affected by climate change may help improve the accuracy of the predictions.

Acknowledgements

The research presented in this chapter was supported in part by the Centre for Risk-Based Community Resilience Planning funded by the US National Institute of Standards and Technology (NIST Financial Assistance Award Number: 70NANB15H044). The views expressed are those of the authors, and may not represent the official position of the sponsor.

References

Akaike, H., 1974. A new look at the statistical model identification. IEEE Trans. Autom. Control AC-19, 716–723.

Asher, M.J., Croke, B.F.W., Jakeman, A.J., Peeters, L.J.M., 2015. A review of surrogate models and their application to groundwater modeling. Water Resour. Res. 51, 5957–5973.

Batts, M.E., Cordes, M.R., Russell, L.R., Shaver, J.R., Simiu, E., 1980. Hurricane wind speeds in the United States. National Bureau of Standards, Report Number BSS-124, US Department of Commerce.

Bjarnadottir, S., Li, Y., Stewart, M.G., 2011. A probabilistic-based framework for impact and adaptation assessment of climate change on hurricane damage risks and costs. Struct. Saf. 33 (3), 173–185.

Booij, N., Holthuijsen, L.H., Ris, R.C., 1996. The SWAN wave model for shallow water. In: Proceedings of the 25th International Conference on Coastal Engineering, Orlando, USA. vol. 1. pp. 668–676.

Bretschneider, C.L., 1972. A non-dimensional stationary hurricane wave model. In: Proceedings of 1972 Offshore Technology Conference, Houston, Texas.

Bunya, S., Dietrich, J.C., Westerink, J.J., Ebersole, B.A., Smith, J.M., Atkinson, H., Jensen, R., Resio, R.A., Luettich, D.T., Dawson, C., Cardone, V.J., Cox, A.T., Powell, M.D., Westerink, H.J., Roberts, H.J., 2010. A high-resolution coupled riverine flow, tide, wind, wind wave, and storm surge model for southern Louisiana and Mississippi. Part I: model development and validation. Mon. Weather Rev. 138, 345–377.

Camargo, S.J., 2013. Global and regional aspects of tropical cyclone activity in the CMIP5 models. J. Climate 26, 9880–9902.

Chavas, D.R., Lin, N., Emanuel, K., 2015. A model for the complete radial structure of the tropical cyclone wind field. Part I: comparison with observed structure. J. Atmos. Sci. 72 (9), 3647–3662.

Contento, A., Chhabra, T., Gardoni, P., Dierer, S., 2017. Analysis of the effects of climate change on insurance against hurricanes. In the 12th Int. Conference on Structural Safety & Reliability (ICOSSAR2017), Vienna, Austria, August 2017.

Contento, A., Xu, H., Gardoni, P., 2018. A physics-based transportable probabilistic model for climate change dependent storm surge. In: Gardoni, P. (Ed.), Handbook of Sustainable and Resilient Infrastructure. Routledge.

Cooper, J.A.G., Pile, J., 2013. The adaptation-resistance spectrum: a classification of contemporary adaptation responses to climate-related coastal change. Ocean Coast. Manag. 94, 90–98.

Dietrich, J.C., Zijlema, M., Westerink, J.J., Holthuijsen, L.H., Dawson, C., Luettich, R.A., Jensen, R.E., Smith, J.M., Stelling, G.S., Stone, G.W., 2011. Modeling hurricane waves and storm surge using integrally-coupled, scalable computations. Coast. Eng. 58, 45–65.

Emanuel, K., 2004. Tropical cyclone energetics and structure. In: Fedorovich, E., Rotunno, R., Stevens, B. (Eds.), Atmospheric Turbulence and Mesoscale Meteorology. Cambridge University Press, Cambridge.

Emanuel, K., Rotunno, R., 2011. Self-stratification of tropical cyclone outflow. Part I: implications for storm structure. J. Atmos. Sci. 68, 2236–2249.

Emanuel, K., Ravela, S., Vivant, E., Risi, C., 2006. A statistical deterministic approach to hurricane risk assessment. Bull. Am. Meteorol. Soc. 87 (3), 299–314.

FEMA, 2005. Hurricane mitigation. In: A Handbook for Public Facilities. Department of Homeland Security, Federal Emergency Management Agency, Mitigation Division, Washington, D.C.

FEMA, 2009a. HAZUS-MH MR4 Hurricane Model Technical Manual. Department of Homeland Security, Federal Emergency Management Agency, Mitigation Division, Washington, DC.

FEMA, 2009b. HAZUS-MH MR4 Flood Model Technical Manual. Department of Homeland Security, Federal Emergency Management Agency, Mitigation Division, Washington, DC.

FEMA, 2012. Multi-Hazard Loss Estimation Methodology Hurricane Model Technical Manual. Department of Homeland Security, Federal Emergency Management Agency, Mitigation Division, Washington, DC.

Gardoni, P. (Ed.), 2017. Risk and Reliability Analysis: Theory and Applications. Springer, Cham.

Gardoni, P., Mosalam, K.M., Der Kiureghian, A., 2002. Probabilistic capacity models and fragility estimates for RC columns based on experimental observations. J. Eng. Mech. ASCE 128 (10), 1024–1038.

Gardoni, P., Guevara-Lopez, F., Contento, A., 2016. The life profitability method (LPM): a financial approach to engineering decisions. Struct. Saf. 63, 11–20.

Georgiou, P.N., 1985. Design Windspeeds in Tropical Cyclone-Prone Regions. PhD thesis, Faculty of Engineering Science, University of Western Ontario, London, Ontario, Canada.

Grace, M.F., Klein, R.W., Liu, Z., 2005. Increased hurricane risk and insurance market responses. J. Insur. Regul. 24 (2), 3–32.

Hofer, L., Gardoni, P., Zanini, M.A., 2018. CAT bond pricing and coverage design against natural perils. In: Gardoni, P. (Ed.), Handbook of Sustainable and Resilient Infrastructure. Routledge.

Holland, G.J., 1980. An analytic model of the wind and pressure profiles in hurricanes. Mon. Weather Rev. 108, 1212–1218.

Holland, G.J., Belanger, J.I., Fritz, A., 2010. A revised model for radial profiles of hurricane winds. Mon. Weather Rev. 138, 4393–4401.
Houston, S.H., Shaffer, W.A., Powell, M.D., Chen, J., 1999. Comparisons of HRD and SLOSH surface wind fields in hurricanes: implications for storm surge modeling. Weather Forecast. 14, 671–686.
IPCC, 2007. Climate models and their evaluation. In: Solomon, S., Qin, D., Manning, M., Chen, Z., Marquis, M., Averyt, K.B., Tignor, M., Miller, H.L. (Eds.), Climate Change 2007: The Physical Science Basis. Contribution of Working Group I to the Fourth Assessment Report of the Intergovernmental Panel on Climate Change. Cambridge University Press, Cambridge and New York, NY, pp. 589–662.
IPCC, 2013. Stocker, T.F., Qin, D., Plattner, G.-K., Tignor, M., Allen, S.K., Boschung, J., Nauels, A., Xia, Y., Bex, V., Midgley, P.M. (Eds.), Climate Change 2013: The Physical Science Basis. Contribution of Working Group I to the Fifth Assessment Report of the Intergovernmental Panel on Climate Change. Cambridge University Press, Cambridge and New York, NY.
Irish, J.L., Resio, D.T., Ratcliff, J.J., 2008. The influence of storm size on hurricane surge. J. Phys. Oceanogr. 38, 2003–2013.
Jaffee, D., Kunreuther, H., Michel-Kerjan, E., 2010. Long-term property insurance. J. Insur. Regul. 29, 167–187.
Jarvinen, B., Lawrence, M., 1985. An evaluation of the SLOSH storm surge model. Bull. Am. Meteorol. Soc. 66, 1408–1411.
Jelesnianski, C.P., Chen, J., Shaffer, W.A., 1992. SLOSH: sea, lake, and overland surges from hurricanes. NOAA Tech. Report NWS 48.
Jia, G., Taflanidis, A.A., 2013. Kriging metamodeling for approximation of high-dimensional wave and surge responses in real-time storm/hurricane risk assessment. Comput. Methods Appl. Mech. Eng. 261–262, 24–38.
Jia, G., Taflanidis, A.A., Nadal-Caraballo, N.C., Melby, J.A., Kennedy, A.B., Smith, J.M., 2016. Surrogate modeling for peak or time-dependent storm surge prediction over an extended coastal region using an existing database of synthetic storms. Nat. Hazards 81 (2), 909–938.
Johnson, D.R., Fischbach, J.R., Ortiz, D.S., 2013. Estimating surge-based flood risk with the coastal Louisiana risk assessment model. J. Coast. Res. Spec. Issue 67, 109–126.
Jolliffe, I.T., 2002. Principal Component Analysis, Series: Springer Series in Statistics, Second ed. Springer, NY.
Kendra, M.D., Xue, X., Xu, J., Wang, N., Kolar, R.L., Geoghegan, K.M., 2017. A coupled model system for hurricanes, storm surge and coastal flooding to support community resilience planning under climate change. In: 12th Int. Conference on Structural Safety & Reliability (ICOSSAR2017), Vienna, Austria, August 2017.
Kepert, J.D., 2010. Slab- and height-resolving models of the tropical cyclone boundary layer. Part I: comparing the simulations. Q. J. R. Meteorol. Soc. 136, 1686–1699.
Kim, S.W., Melby, J.A., Nadal-Caraballo, N.C., Ratcliff, J., 2015. A time-dependent surrogate model for storm surge prediction based on an artificial neural network using high-fidelity synthetic hurricane modelling. Nat. Hazards 76 (1), 565–585.
Knutson, T.R., Sirutis, J.J., Zhao, M., Tuleya, R.E., Bender, M., Vecchi, G.A., Villarini, G., Chavas, D., 2015. Global projections of intense tropical cyclone activity for the late twenty-first century from dynamical downscaling of CMIP5/RCP4.5 scenarios. J. Climate 28, 7203–7224.
Kossin, J.P., Emanuel, K.A., Camargo, S.J., 2016. Past and projected changes in western North Pacific tropical cyclone exposure. J. Climate 29, 5725–5739.
Langousis, A., Veneziano, D., 2009. Theoretical model of rainfall in tropical cyclones for the assessment of long-term risk. J. Geophys. Res. 114, D02106.

LaRow, T.E., Lim, Y.-K., Shin, D.W., Chassignet, E.P., Cocke, S., 2008. Atlantic basin seasonal hurricane simulations. J. Climate 21, 3191–3206.
Lee, J.Y., Ellingwood, B.R., 2017. A decision model for intergenerational life-cycle risk assessment of civil infrastructure exposed to hurricanes under climate change. Reliab. Eng. Syst. Saf. 159, 100–107.
Lee, K.H., Rosowsky, D.V., 2007. Synthetic hurricane wind speed records: development of a database for hazard analysis and risk studies. ASCE, Nat. Hazard. Rev. 8 (2), 23–34.
Li, Y., van de Lindt, J., Dao, T., Bjarnadottir, S., Ahuja, A., 2012. Loss analysis for combined wind and surge in hurricanes. Nat. Hazard. Rev. 13, 1–10.
Lin, N., Emanuel, K., Oppenheimer, M., Vanmarcke, E., 2012. Physically based assessment of hurricane surge threat under climate change. Nat. Clim. Chang. 2 (6), 462–467.
Lin, N., Emanuel, K., Vanmarcke, E., 2014. Hurricane risk analysis: a review on the physically-based approach. In: Deodatis, G., Ellingwood, B.R., Frangopol, D.M. (Eds.), Safety, Reliability, Risk and Life-Cycle Performance of Structures and Infrastructures. CRC Press, Boca Raton, FL, pp. 1291–1297.
Lonfat, M., Rogers, R., Marchok, T., Marks, F.D., 2007. A parametric model for predicting hurricane rainfall. Mon. Weather Rev. 135, 3086–3097.
Mattocks, C., Forbes, C., 2008. A real-time, event-triggered storm surge forecasting system for the state of North Carolina. Ocean Model. 25, 95–119.
Mizuta, R., Yoshimura, H., Murakami, H., Matsueda, M., Endo, H., Ose, T., Kamiguchi, K., Hosaka, M., Sugi, M., Yukimoto, S., Kusunoki, S., Kitoh, A., 2012. Climate simulations using MRI-AGCM3.2 with 20-km grid. J. Meteorol. Soc. Jpn. 90A, 233–258.
Mudd, L., Wang, Y., Letchford, C., Rosowsky, D., 2014. Assessing climate change impact on the US east coast hurricane hazard: temperature, frequency, and track. Nat. Hazard. Rev. 15 (3), 1–11.
Mudd, L., Rosowsky, D., Letchford, C., Lombardo, F., 2017. Joint probabilistic wind–rainfall model for tropical cyclone hazard characterization. J. Struct. Eng. 143(3) 04016195.
Murphy, C., Gardoni, P., McKim, R. (Eds.), 2018. Climate Change and Its Impacts. Springer, Cham.
Neumann, C.J., 1991. The National Hurricane Center Risk Analysis Program (HURISK). In: NOAA Technical Memorandum NWS NHC 38. National Oceanic and Atmospheric Administration (NOAA), Washington, DC.
Olshansky, R.B., 2018. Recovery after disasters: how adaptation to climate change will occur. In: Murphy, C., Gardoni, P., McKim, R. (Eds.), Climate Change and Its Impact: Risks and Inequalities. Springer, Cham.
Ou Yang, C., 2010. Managing Catastrophic Risk by Alternative Risk Transfer Instruments. Publicly Accessible Penn Dissertations, p. 220.
Phadke, A.C., Martino, C.D., Cheung, K.F., Houston, S.H., 2003. Modeling of tropical cyclone winds and waves for emergency management. Ocean Eng. 30, 553–578.
Powell, M.D., Vickery, P.J., Reinhold, T.A., 2003. Reduced drag coefficient for high wind speeds in tropical cyclones. Nature 422 (6929), 279–283.
Powell, M., Soukup, G., Cocke, S., Gulati, S., Morisseau-Leroy, N., Hamid, S., Dorst, N., Axe, L., 2005. State of Florida hurricane loss projection model: atmospheric science component. J. Wind Eng. Ind. Aerodyn. 93 (8), 651–674.
Resio, D.T., Westerink, J.J., 2008. Modeling the physics of storm surges. Phys. Today 61 (9), 33–38.
Roland, A., Cucco, A., Ferrarin, C., Hsu, T.-W., Liau, J.-M., Ou, S.-H., Umgiesser, G., Zanke, U., 2009. On the development and verification of a 2-D coupled wave-current model on unstructured meshes. J. Mar. Syst. 78, 244–254. Suppl. 1.
Russell, L.R., 1971. Probability distributions for hurricane effects. J. Waterw. Harb. Coast. Eng. Div. 97, 139–154.

Scawthorn, C., Flores, P., Blais, N., Seligson, H., Tate, E., Chang, S., Mifflin, E., Thomas, W., Murphy, J., Jones, C., Lawrence, M., 2006. Hazus-MH flood loss estimation methodology. II: damage and loss assessment. Nat. Hazard. Rev. 7 (2), 72–81.
Schmidt, A.M., Guttorp, P., O'Hagan, A., 2011. Considering covariates in the covariance structure of spatial processes. Environmetrics 22 (4), 487–500.
Schwerdt, R.W., Ho, F.P., Watkins, R.W., 1979. Meteorological criteria for standard project hurricane and probable maximum hurricane wind fields, Gulf and East Coasts of the United States. NOAA technical report NWS 23, US Department of Commerce.
Stevenson, A. (Ed.), 2010. Oxford Dictionary of English. third ed, Oxford University Press, Oxford.
Stewart, M.G., Val, D., Bastidas-Arteaga, E., O'Connor, A., Wang, X., 2014. Climate adaptation engineering and risk-based design and management of infrastructure. In: Frangopol, D.M., Tsompanakis, Y. (Eds.), Maintenance and Safety of Aging Infrastructure. Taylor and Francis Publishers, pp. 641–684.
Strachan, J., Vidale, P.L., Hodges, K., Roberts, M., Demory, M.-E., 2013. Investigating global tropical cyclone activity with a hierarchy of AGCMs: the role of model resolution. J. Climate 26, 133–151.
Thompson, E.F., Cardone, V.J., 1996. Practical modeling of hurricane surface wind fields. J. Waterw. Port Coast. Ocean Eng. 122 (4), 195–205.
Tuleya, R.E., DeMaria, M., Kuligowski, R.J., 2007. Evaluation of GFDL and simple statistical model rainfall forecasts for U.S. landfalling tropical storms. Weather Forecast. 22, 56–70.
Vickery, P.J., Twisdale, L.A., 1995. Prediction of hurricane wind speeds in the US. J. Struct. Eng. 121, 1691–1699.
Vickery, P.J., Skerlj, P.F., Steckley, A.C., Twisdale, L.A., 2000a. Hurricane wind field model for use in hurricane simulations. ASCE, J. Struct. Eng. 126 (10), 1203–1221.
Vickery, P.J., Skerjl, P.F., Twisdale, L.A., 2000b. Simulation of hurricane risk in the U.S. using empirical track model. J. Struct. Eng. 126, 1222–1237.
Vickery, P.J., Masters, F.J., Powell, M.D., Wadhera, D., 2009a. Hurricane hazard modeling: the past, present, and future. J. Wind Eng. Ind. Aerodyn. 97 (7–8), 392–405.
Vickery, P.J., Wadhera, D., Powell, M.D., Chen, Y., 2009b. A hurricane boundary layer and wind field model for use in engineering applications. J. Appl. Meteorol. Climatol. 48, 381–405.
Westerink, J.J., Luettich, R.A., Blain, C.A., Scheffner, N.W., 1994. ADCIRC: an advanced three-dimensional circulation model for shelves, coasts and estuaries. Report 2: Users Manual for ADCIRC-2DDI. Department of the Army, US Army Corps of Engineers.
Westerink, J.J., Luettich, R.A., Feyen, J.C., Atkinson, J.H., Dawson, C., Roberts, H.J., Powell, M.D., Dunion, J.P., Kubatko, E.J., Pourtaheri, H., 2008. A basin to channel scale unstructured grid hurricane storm surge model applied to southern Louisiana. Mon. Weather Rev. 136 (3), 833–864.
Xu, H., Gardoni, P., 2018. Improved latent space approach for modelling non-stationary spatial–temporal random fields. Spat. Stat. 23, 160–181.
Zhao, M., Held, I.M., Lin, S.-J., Vecchi, G.A., 2009. Simulations of global hurricane climatology, interannual variability, and response to global warming using a 50-km resolution GCM. J. Climate 22, 6653–6678.

Further Reading

Bornn, L., Shaddick, G., Zidek, J.V., 2012. Modeling nonstationary processes through dimension expansion. J. Am. Stat. Assoc. 107 (497), 281–289.
Burnecki, K., Kukla, G., 2003. Pricing of zero-coupon and coupon CAT bonds. Appl. Math. 30, 315–324.

Fouedjio, F., Desassis, N., Romary, T., 2015. Estimation of space deformation model for non-stationary random functions. Spat. Stat. 13, 45–61.
Fuglstad, G.-A., Simpson, D., Lindgren, F., Rue, H., 2015. Does non-stationary spatial data always require non-stationary random fields? Spat. Stat. 14 (Part C), 505–531.
Härdle, W.K., Cabrera, B.L., 2010. Calibrating CAT bonds for Mexican earthquakes. J. Risk Insur. 77 (3), 625–650.
Hubbert, G.D., McInnes, K.L., 1999. A storm surge inundation model for coastal planning and impact studies. J. Coast. Res. 15 (1), 168–185.
Katzfuss, M., 2013. Bayesian nonstationary spatial modeling for very large datasets. Environmetrics 24 (3), 189–200.
Lindgren, F., Rue, H., Lindström, J., 2011. An explicit link between Gaussian fields and Gaussian Markov random fields: the stochastic partial differential equation approach. J. R. Stat. Soc. Series B Stat. Methodology 73 (4), 423–498.
Mateu, J., Fernández-Avilés, G., Montero, J.M., 2013. On a class of non-stationary, compactly supported spatial covariance functions. Stoch. Env. Res. Risk A. 27 (2), 297–309.
Nychka, D., Wikle, C., Royle, J.A., 2002. Multiresolution models for nonstationary spatial covariance functions. Stat. Model. 2 (4), 315–331.
Paciorek, C.J., Schervish, M.J., 2006. Spatial modelling using a new class of nonstationary covariance functions. Environmetrics 17 (5), 483–506.
Reich, B.J., Eidsvik, J., Guindani, M., Nail, A.J., Schmidt, A.M., 2011. A class of covariate-dependent spatiotemporal covariance functions. Ann. Appl. Stat. 5 (4), 2425–2447.
Risser, M.D., Calder, C.A., 2015. Regression-based covariance functions for nonstationary spatial modelling. Environmetrics 26 (4), 284–297.
Sampson, P.D., Guttorp, P., 1992. Nonparametric estimation of nonstationary spatial covariance structure. J. Am. Stat. Assoc. 87 (417), 108–119.
van Vuuren, D.P., Edmonds, J., Kainuma, M., Riahi, K., Thomson, A., Hibbard, K., Hurtt, G.C., Kram, T., Krey, V., Lamarque, J.-F., Masui, T., Meinshausen, M., Nakicenovic, N., Smith, S.J., Rose, S.K., 2011. The representative concentration pathways: an overview. Clim. Change 109, 5–31.
Vanmarcke, E., 2010. Random Fields: Analysis and Synthesis. World Scientific, Singapore.